

Evaluation of Bogie Bolster Centre Plate and Side Bearing under Vertical Static Loads through Finite Element (FEA) Modelling

IP Artha Wirawan^{1,2}, IDG Ary Subagia^{1,2*}, IK Adi Atmika¹, A Rohman Farid²

Program Study of Mechanical Engineering, Udayana University, Bukit Jimbaran, Badung, Bali, Indonesia
 Metarial Engineering Laboratory, Faculty of Engineering, Buit Jimbaran Badung, Bali, Indonesia
 3PT. Indonesian Railway Company (INKA), Kota Madiun, Jawa Timur, Indonesia arsubmt@unud.ac.id

Received 2025-07-21, Revised 2025-09-25, Accepted 2025-10-30, Available Online 2025-10-30, Published Regularly October 2025

ABSTRACT

The bolster is a primary structural component in a railroad bogie, vital for transferring vertical and dynamic loads from the car body to the wheels. This study investigates the mechanical properties of bearings made from ASTM A148 Grade 80-50 material under vertical static loading conditions. The simulation was performed using Finite Element Analysis (FEA) with a student edition of the software, implementing nonlinear static analysis. The research utilized a tetrahedral mesh and employed a Newton-Raphson iteration method. Three variables were analyzed, two of which are dependent: Von Mises Stress (VMS) and total deformation resulting from loading conditions. The independent variable is the load value as per AAR M-202 criteria. The study produced two load values: P1 = 536010.7 N and P2 = 854058.8 N. The simulation results indicate that the peak average stress in the critical region is 305.58 MPa, which remains below the material's yield strength of 390 MPa. The maximum elastic deflection recorded is 0.102 mm, significantly below the permissible limit set by AAR M-202 regulations. Bogie bolsters that meet ASTM A148 Grade 80-50 standards are reliable for static loads and are provided with a safety factor in accordance with AAR M-202 regulations.

Keywords: Bogie Bolster; Deflection; Finite Element Method; Static Loading; Train; Stress-Strain

INTRODUCTION

The train is one of the most widely used forms of public transportation. The advantages of this mode include speed, affordability, and high carrying capacity. However, trains became part of the "human-machine-environment." This is an important motto that leads to the operational sustainability of transportation modes like trains. Accidents are one of the consequences of negligence involving humans, vehicles, and the environment. Train accidents can be caused by external or internal factors, or a combination of both [1], [2], [3]. Accidents caused by external factors include human error, damage to railroad tracks, signal system failures, and unsafe conditions at railroad crossings. Additionally, environmental factors such as heavy rain, floods, and significantly reduced visibility contribute to a decline in operational safety levels [4]. The presence of foreign objects or wildlife on the tracks also increases the risk of accidents [5], necessitating strict monitoring and maintenance of railroad infrastructure, as well as adequate training for operators [6]. Internal factors, including engine failures and issues related to the construction and structure of the railroad tracks, also contributed to the decline in operational quality. A bogie is the undercarriage of a rail vehicle structure. The bogie supports various loads, including the car body and moving components such as wheels, suspension systems, braking systems, and other propulsion equipment. The function of a bogie is to control the train's stable movement, follow the track's curves, and dampen vibrations and shock forces

during the journey. Many train accidents involve damage to the bogie, such as cracks in the frame, damage to the wheel axles, or wheel failure [7]. In addition to mechanical damage, poor track conditions, such as cracked or uneven rails, can also cause the bogie to derail or come off the tracks, potentially leading to serious accidents. The vertical load on a train comes from its weight (dead load) and operational loads, which include passengers, cargo, and additional forces generated during acceleration and braking. Proper analysis of these loads can prevent material fatigue and structural cracks. FEA is a numerical method used to assess the behavior of complex structures by dividing them into smaller elements. In the analysis of bogie bolsters, FEA has proven its effectiveness in simulating actual loading conditions and comprehensively evaluating structural strength [8]. Theoretically, FEA is highly effective for analyzing and verifying the safety of bogie bolster designs under vertical static loading, and extensive research has been conducted on bolster loading characteristics [9]. On the other hand, the finite element method is widely used because it is inexpensive and efficient in analyzing complex structures [10]. This section presents a static load analysis on the bolster used for the temporary bogie lifter made of JIS G 3192 material [12]. This analysis emphasizes structural strength, including stress, strain, and bearing deformation on the temporary bogie and temporary bogie lifter, using Finite Element Analysis (FEA) with Tansy software. Additionally, we compare the structural performance of the temporary bogie design with that of the temporary bogie lifter. The results indicate that the temporary bogie lifting design has superior capabilities, as it can withstand static loads of up to 10 tons. Furthermore, FEA applications have been used to analyze static loading under various conditions, including vertical loads on the UGL 60 FT flatcar bogie. The findings indicate that the bogie structure remains safe for use on flat tracks because the maximum stress around the springs is still below the material's yield strength of 262 MPa [13]. Additionally, research using FEA software was conducted to evaluate the strength limits of the adapter frame for the bogie bolster according to UIC 615-4 standards, considering various load variations, including longitudinal, vertical, and lateral loads [14]. The analysis indicated that the maximum stress obtained under external loads was 91.244 MPa, with a maximum deformation of 2.7855 mm. These values remained below the material's yield strength, indicating that the design is safe and suitable for use. Next, research was conducted to assess the impact of multidirectional static loads in vertical, horizontal, and lateral directions on the movement and braking of the train [15]. Subsequently, testing was performed on the dynamic response and lateral stability of the bogie according to AAR MSRP C standards [16]. This testing illustrates the importance of numerical analysis in determining critical areas related to stress, strain, and deflection before field testing. Thereafter, dynamic vibration analysis was performed using Finite Element Analysis (FEA) [17]. The results provided evidence that FEA can accurately predict stress and strain distribution through 3D modeling [4]. The utilization of FEA for analyzing stress and strain distribution contributes to ensuring operator safety [18]. Other studies have shown a high level of accuracy in validating FEA for predicting deformation and stress on bearings [19]. Given the accuracy of FEA results in analyzing the maximum stress contours on high-speed train bogies, it is recommended for use in yield strength (YS) testing of SS400 material, in accordance with EN 13749 and ASTM A148 Grade 80-50 standards, as well as AAR M-202 [20]. An intriguing aspect of the bogie bolster testing is that the yield strength was not reached under static loading, even though the SS400 material was adapted to the EN 13749 standard. This phenomenon poses specific challenges for bogies, particularly concerning the static loading of ASTM A148 Grade 80-50 material, which is recommended as a substitute for SS400 according to AAR M-202 standards. This discussion is important because the distribution of static stress, especially at critical points, is susceptible to permanent deformation. Additionally, there is a lack of information regarding static loading, potential permanent deformation, and stress patterns in key areas to assess whether bolster components made from ASTM A148 Grade 80-50 can meet the static stress standards outlined in AAR M-

202. Therefore, further research using Finite Element Analysis (FEA) is needed. This study evaluates train bogies manufactured by PT Kereta Api Indonesia (INKA). This research aims to analyze and evaluate the stress and deformation experienced by the bogie when subjected to a static vertical load applied to the bolster, in accordance with ASTM A148 Grade 80-50 standards. Testing was conducted using simulations with FEA software. The analysis results are presented in the form of images, illustrating the minimum and maximum stress distribution as well as the deformation resulting from the vertical load.

.

MANUFACTURE AND SIMULATION

Bolster of Bogie Train

An important part of the traditional train bogie design is the bolster, which serves as the main bridge between the bogie and the train body. This element ensures safe, stable, and comfortable operation by distributing the load, allowing bogie rotation, and working with the suspension system. According to the needs of various railroad vehicles, railroad bogie bearings can be divided into the following categories: high-speed railroad bearings (HSTB), heavy-duty railroad bearings (HDTB), also known as freight car bearings, and urban railroad bearings (URTB) [21]. Figure 1 shows the main components of a freight car bogie. One of the main design principles of a bogie is its ability to evenly transfer the load from the train to the rails, thereby reducing wear on the wheels and rails and minimizing the effects of vibration [22].

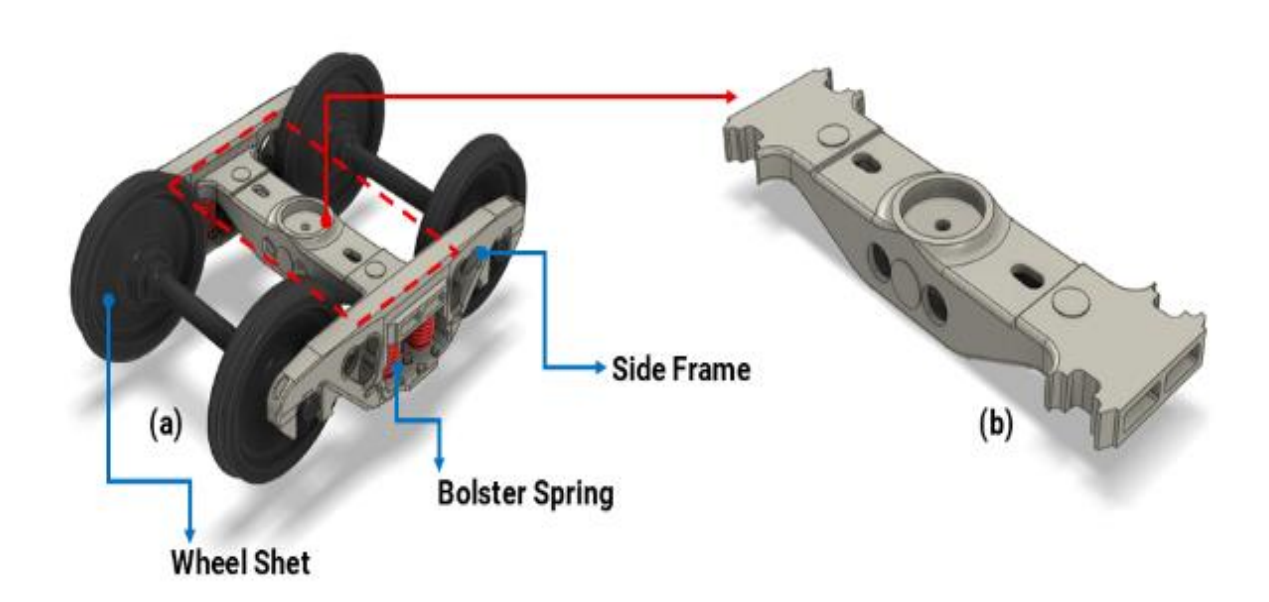


Figure 1. 3D Design of Main Bogie Component (a) Bogie, (b) Bolster

Research Flowchart

This study begins with a comprehensive literature review, gathering insights from prior research relevant to the problem under investigation. Following this, a 3D model of the railway bogie bolster was created using CAD software, based on actual dimensions. The material properties of ASTM A148 Grade 80-50—including density, Young's Modulus, Poisson's Ratio, and yield stress—were defined and assigned to the model.

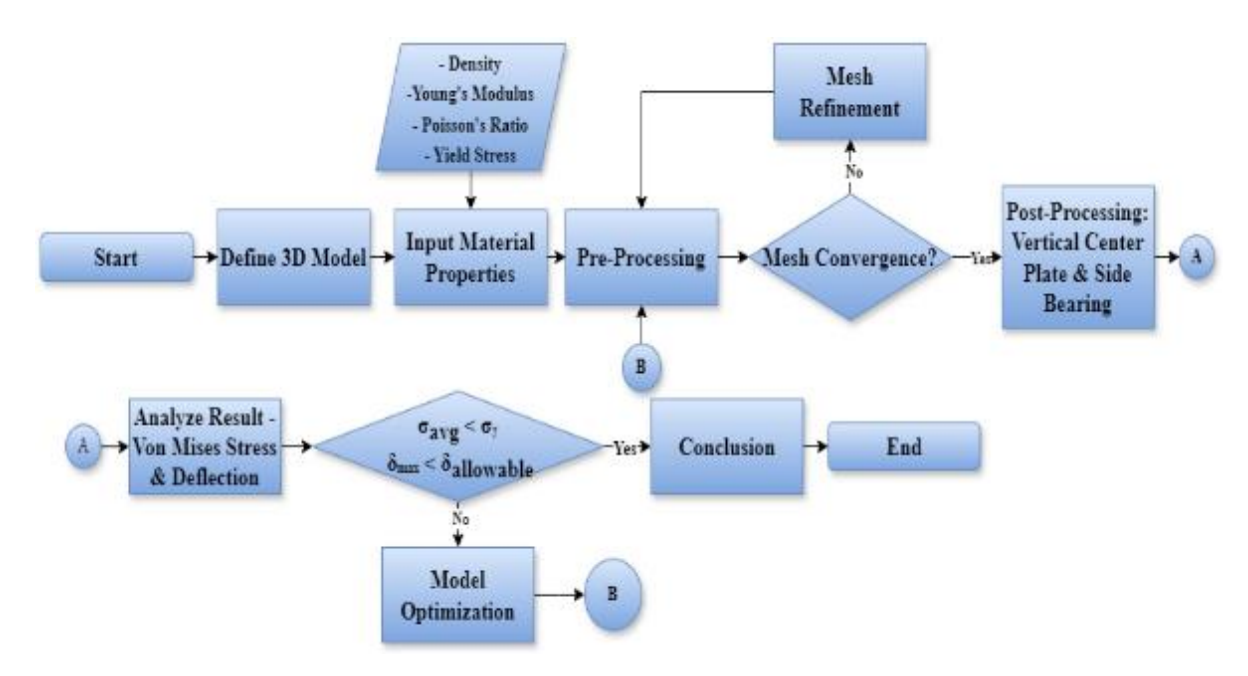


Figure 2. Research Flowchart

In the pre-processing stage of the finite element analysis, the bolster model was discretized into smaller finite elements. Each element is governed by a local stiffness matrix [K] and force vector [F], formulated using the Galerkin weak form to accurately represent structural behavior under applied loads. A mesh convergence analysis was then performed to verify that the simulation results remained consistent across different mesh sizes. This process ensures an optimal balance between solution accuracy and computational cost. If convergence was not achieved, further mesh refinement was conducted to improve result reliability.

Once mesh convergence was established, the simulation proceeded to the post-processing phase, where the model was subjected to different types of loading, namely Vertical Centre Plate Load (VCPL), Vertical Side Bearing Load (VSBL), and Transverse Load (TL). Each load case was applied sequentially to observe its effect on the structure.

This analysis refers to two key criteria:

$$\sigma_{avg} < \sigma_{y}$$
 (1)

$$\delta_{max} < \delta_{allowable}$$
 (2)

Where σ_{avg} explains the average stress of the critical area under loading conditions, and σ_y is the material's yield stress. Meanwhile, δ_{max} is the maximum deformation obtained from the simulation, and $\delta_{allowbale}$ is the allowable deflection limit based on AAR M-202 standards. If either condition was not met, the design optimization step was carried out by adding fillets in stress-concentrated areas to reduce the peak stress of the structure.

Material ASTM A148 Grade 80-50

The car bogie is designed to withstand dynamic and static loads during train operation. Therefore, the use of materials capable of maintaining the durability and safety of the bogie frame structure is critical. In its development, many types of materials have been applied as bogies, including the most common, such as B and C class cast steel, as defined in the AAR M-202 standard, with chemical and mechanical properties shown in Tables 1 and 2 [23].

Bogie bearings are typically made from materials that meet ASTM A148 Grade 80-50 standards, as well as those that meet AAR M202 standards, due to the advantageous properties outlined in Table 3. A comparison of the material characteristics that meet AAR M202 with those that meet ASTM A148 Grade 80-50 shows that AAR M202 materials (see Tables 1 and 2) are generally less suitable for critical requirements in the manufacture of railroad bogie bearings.

Table 1. Chemical Composition of Cast Steel for Bolster AAR M202

Material Grade	C ≤	Si ≤	Mn≤	P ≤	S ≤	Cu≤	Ni≤	Cr≤	Mo≤
Class B	0.28	0.40	1.00	0.030	0.030	0.30	0.30	-	-
Class C	0.28	0.40	1.50	0.030	0.030	0.30	0.35	0.30	0.30

Table 2. Mechanical properties of Cast Steel for Bolster AAR M202

Material Grade	Class B	Class C
Tensile strength	≥485	≥620
Yield Strength	≥260	≥415
Elongation Rate	≥24	≥22
Reduction rate in the section	≥36	≥45
Impact absorption	≥20(-7°C)	≥20(-18°C)

Table 3. Mechanical Properties of ASTM A148 Gr 80-50

Material Grade	Value
Density (kg/m³)	113
Young's Modulus (GPa)	190
Poisson's Ratio	0.29
Tensile Ultimate Strength (MPa)	630
Tensile Yield Strength (MPa)	390

Loading Test Condition

Figure 3a illustrates the loading mechanism for the side bearings and center plate on the bogie, following AAR M-202 standards. Figure 3b provides a free body diagram of the structure, while Figures 3c–3f show the load on the center plate, F_{sb1} and F_{sb2} , positioned 584.2 mm from the center plate. The forces applied to the structure are represented as F_{sb1} and F_{sb2} x. The reactions to the load forces at each support are indicated in two dimensions as R_{Ix} , R_{Iy} , R_{2x} , and R_{2y} . This approach ensures that any deformation observed during testing is not attributed to other loads.

The equilibrium conditions for these loading scenarios can be mathematically expressed as:

1. Equilibrium of forces in the x-direction

$$\sum F_x = 0 \Rightarrow R1_x + R2_x - F_{sb1x} - F_{cpx} - F_{sb2x} = 0$$
(3)

2. Equilibrium of forces in the y-direction

$$\sum F_{\nu} = 0 \Rightarrow R1_{\nu} + R2_{\nu} = 0 \tag{4}$$

3. Moment equilibrium about the left and right support

$$\sum M_{R1} = 0 \Rightarrow F_{sb1x} \cdot a - F_{cpx} \cdot b - F_{sb2x} \cdot c + R_{2x} \cdot d = 0$$

$$\tag{5}$$

$$\sum M_{R2} = 0 \Rightarrow F_{sb2x} \cdot (d - c) - F_{cpx} \cdot (d - b) - F_{sb1x} \cdot (d - a) + R_{1x} \cdot d = 0$$
 (6)

"Here, a, b, and c represent the distances between a support (R), while d denotes the total length between the two supports."

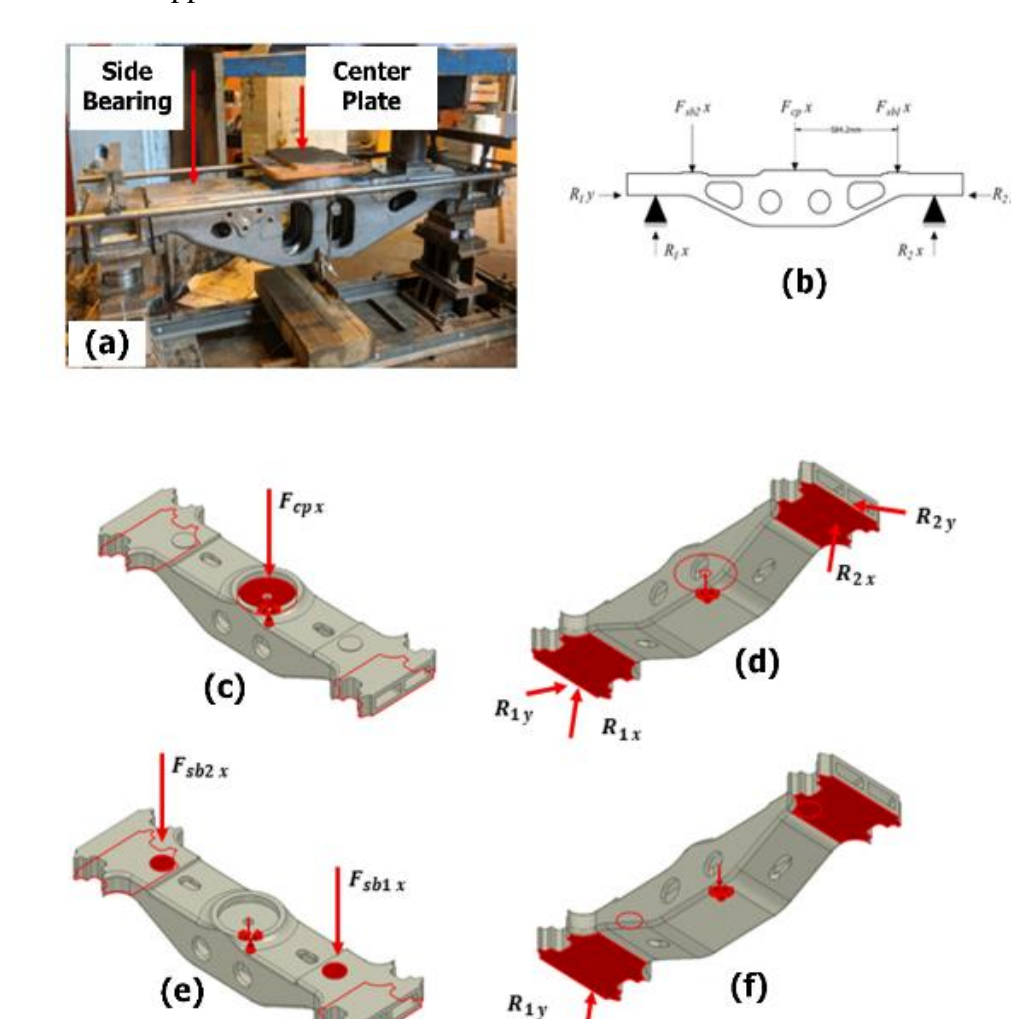


Figure 3. (a) Illustration of a physical testing condition; (b) Free body diagram of the loading with the boundary condition applied in FEA software; (c) Loading center plate; (d) Fixed support center plate; (e) Loading side bearing; (f) Fixed support side bearing.

The applied load values for VCPL and VSBL, based on the AAR M-202 standard, are detailed in Table 4, along with the allowable maximum deviations.

Table 4. Test Loading Values

Items	Code	Load (N)	Deviation Maximum (mm)
Vartical Cantra Plata	P1	536010.7	2.667
Vertical Centre Plate	P3	1027500	0.635
Vartical Side Decrine	P1	536010.7	1.778
Vertical Side Bearing	P2	854058.5	0.635

Formulation of the Finite Element Analysis

Finite Element Analysis (FEA) is a computational method utilized to address complex mechanical challenges by partitioning a physical model into smaller, manageable components known as finite elements ^[24-25]. This technique has demonstrated high efficiency and accuracy in the analysis of large structures, such as train bogies ^[26-27]. FEA integrates mathematical calculations of displacement, strain, and stress that arise from both static and dynamic loading conditions. Figure 4 depicts the analysis of a railroad bogie subjected to a static vertical load on each bearing in a three-dimensional model. In these analyses, the selection of structural meshing is critical, as it can significantly impact the resulting data. In this instance, tetrahedral modeling was chosen to mitigate singularities in the calculations.

The general form of the equilibrium equation in FEA states that the internal resisting force generated by displacement ($K \cdot u$) is equal to the applied external force (F), as shown in equation (7).

$$K \cdot u = F \tag{7}$$

Each element in the model contributes to the overall stiffness of the structure. For solid 3D elements (e.g., tetrahedral), the local stiffness matrix K_e is defined as

$$K_e = \int_{V_o} B^T \cdot D \cdot BdV \tag{8}$$

The assumption that a material behaves in a linear, elastic, and isotropic manner facilitates the definition of the stress-strain relationship. This relationship is essential for comprehending how materials respond to different loading conditions, allowing for the prediction of deformation and potential structural failure. Consequently, it plays a vital role in ensuring safety and reliability in design.

$$\sigma = D \cdot \varepsilon \tag{9}$$

In this context, K represents the global stiffness matrix of the entire structure, while the other symbols denote the following: (u) the nodal displacement vector, F the external nodal force vector, V_e the volume of the element, B the strain displacement matrix, D the elasticity matrix, σ the stress vector, ε the strain vector, and D the elastic stiffness matrix for a 3D isotropic material.

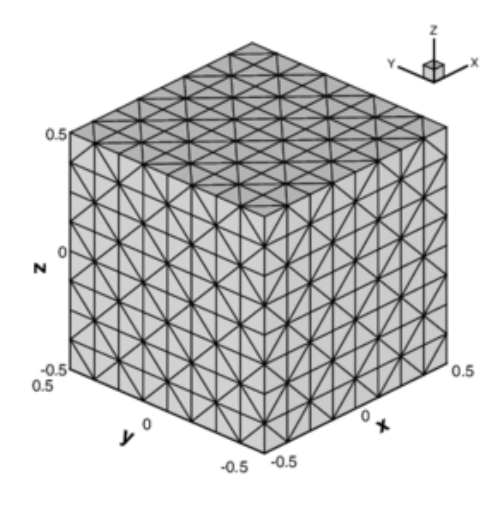


Figure 4. 3D Solid Tetrahedral Elements Mesh

Mesh Convergence

The quality and accuracy of the finite element analysis (FEA) of a structure are influenced by the shape and type of the mesh, as well as the number of nodes. In this analysis, a tetrahedral mesh ^[28] with an initial size of 10 mm was selected. During the convergence process, the mesh size was adjusted, ranging from 6 mm to 1 mm. Figures 5a and 5b illustrate the general shape of the refined mesh. Based on the convergence results, a final mesh size of 2 mm was chosen, as demonstrated by the convergence graph in Figure 5(c). Table 5 shows the convergence of the tetrahedral mesh of the bolster bogie structure.

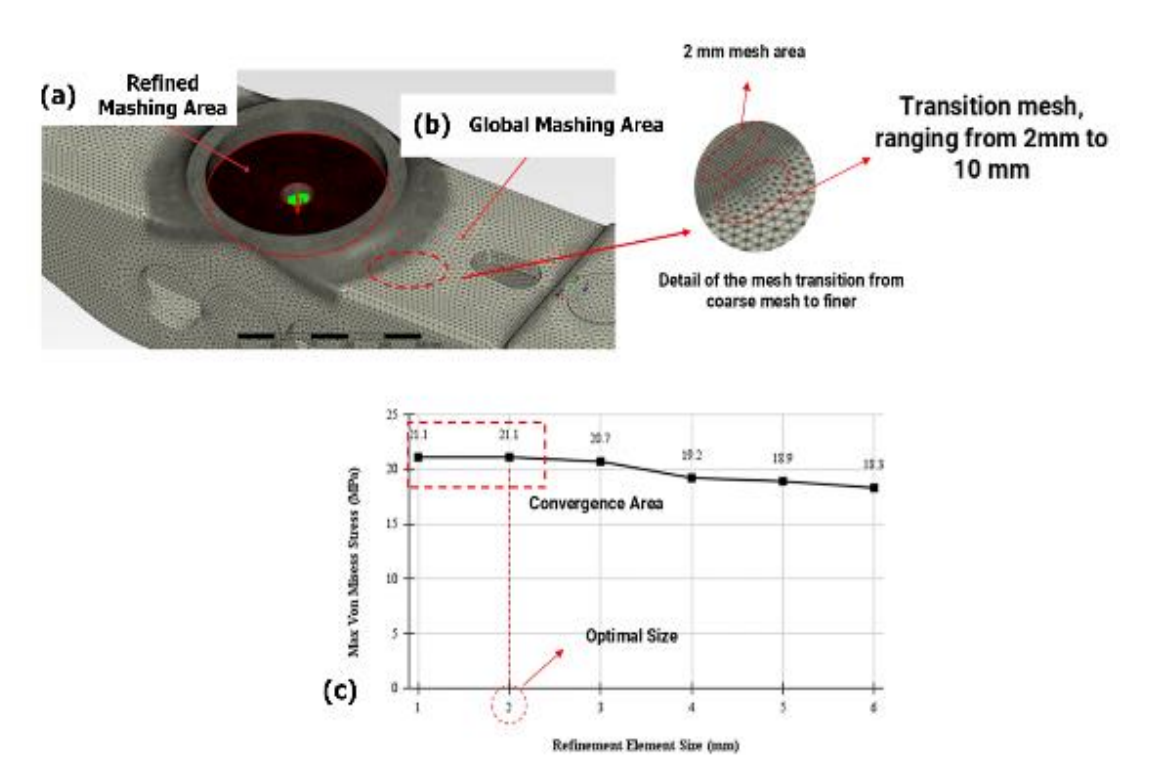


Figure 5. Mesh area of (a) 10 mm global mesh, (b) 6-2 mm refined mesh, (c) Convergence Graph

Table 5. Mesh Convergence Data

Refinement Element Size (mm)	Max Von Misses Stress (MPa)
6	18.3
5	18.9
4	19.2
3	20.7
2	21.1
1	21.2

RESULTS AND DISCUSSION

Vertical Centre Plate

Finite Element Analysis (FEA) is recognized as a method for analyzing complex and large-scale structures. The measurement results yielded precise values for the mechanical characteristics of this structure. This study used FEA to test the mechanical properties of the bogie bolster, focusing on stress and deformation. Analysis of these test results yielded the results illustrated in Figure 6. Figures 6a and 6b present the simulation results obtained from vertical loading P1 and P3 on the Vertical Center Plate (VCP). The findings reveal critical

stress concentrations, according to the Von Misses stress criterion, occurring in the area below the bearing near the fixed support application (as indicated by the red circle). As a result, this area was identified as a critical zone. The calculated average stress value (σ_{avg}) was determined to be 196.09 MPa for P1 loading and 305.58 MPa for P3 loading, respectively. It was observed that the stress contours for both loads, P1 and P3, widened as the magnitude of the load increased. This observation aligns with the research findings of other researchers, such as ^[16], ^[17], ^[18], ^[29], ^[30], ^[31], ^[32]. However, consistent with previous studies, plastic deformation did not occur because the average stress (σ_{avg}) calculated in both scenarios remained below the material's yield strength (σ_y). The results are detailed in Tables 6 and 7.

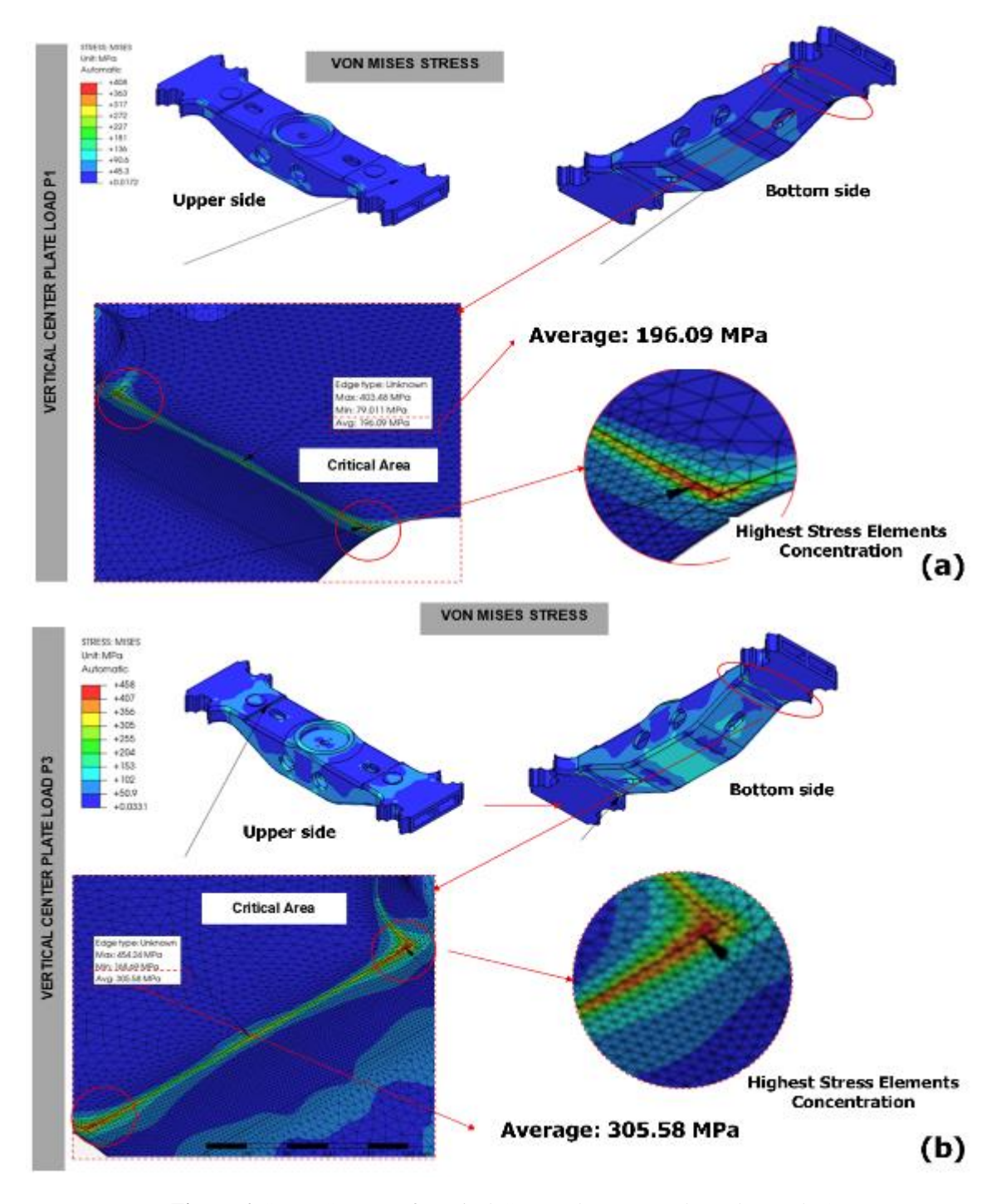


Figure 6. Stress Contour of Vertical Centre Plate (a) Load P1, (b) Load P3

Figures 7a and 7b depict the deformation contours for loads P1 and P2. The figures show that the highest deformation at the Vertical Control Point (VCP) occurs at the center of the plate, indicated by the red color in a square inset, which corresponds to the point of load application. As the applied load increases from P1 to P3, the deformation contours expand significantly. This trend suggests a structural response that increases with the load magnitude, consistent with findings from other studies [$^{16], [17], [18], [29]}$. Under the P1 loading condition, the maximum recorded deformation is $\delta_{max} = 0.482$ mm, while under the P3 loading condition, the maximum observed deformation is $\delta_{max} = 0.926$ mm. Other research corroborates this trend, indicating that the cushion structure undergoes increased local bending with larger loads.

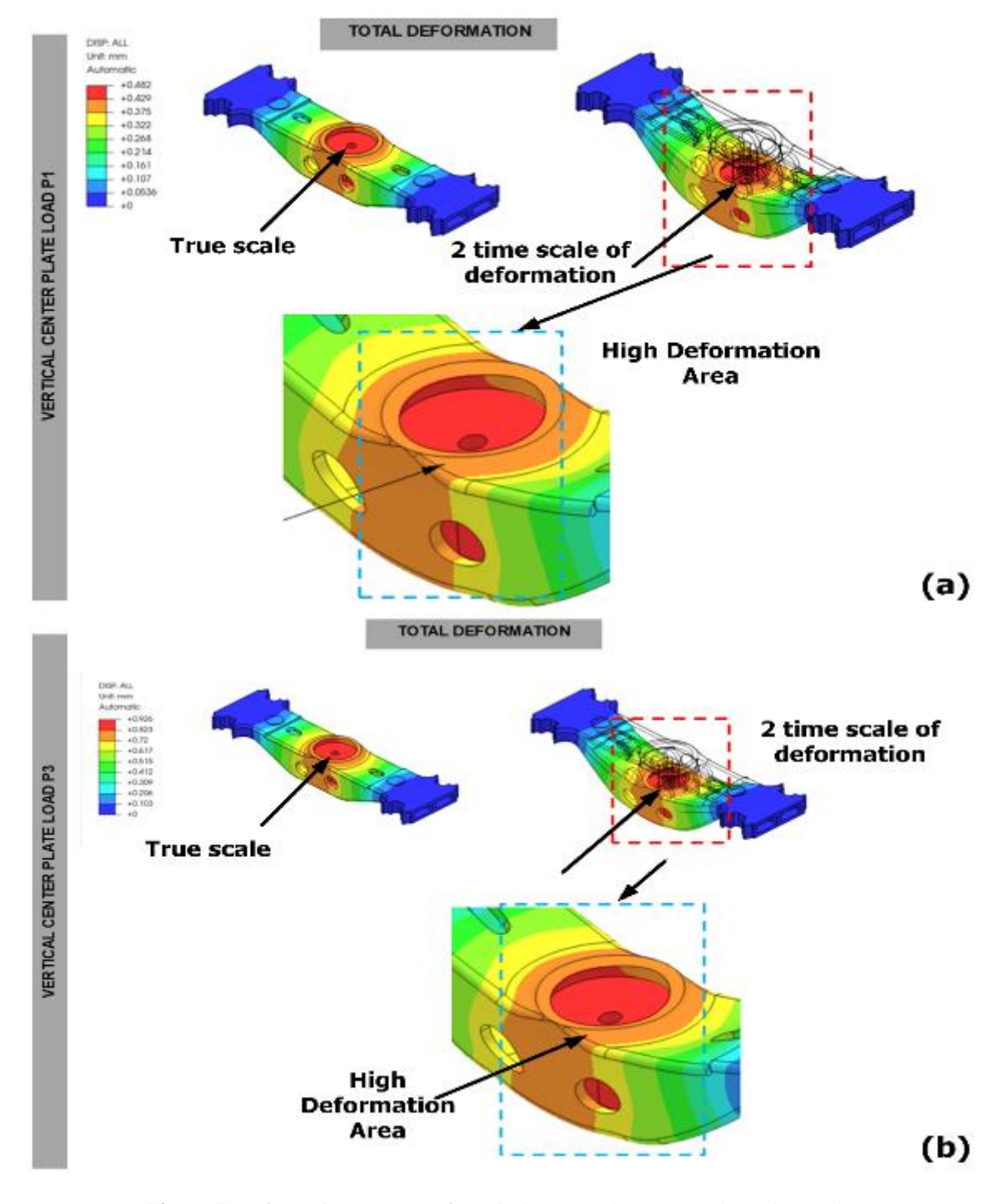


Figure 7. Deformation Contour of Vertical Centre Plate (a) Load P1, (b) Load P3

Vertical Side Bearing

Another aspect of the testing conducted on the bogie bolster involves loading on the vertical side bearings, which aims to determine material characteristics in accordance with ASTM A148 Gr 80-50 standards and adheres to AAR M-202 standards. Loading is applied by P1 and P2 at the Vertical Side Bearing (VSB). The simulation results indicate that the critical stress concentration matches the results obtained from the Vertical Compression Plate (VCP); however, the VSB reveals that the critical area is more concentrated in the middle of that edge, as illustrated in Figures 8a and 8b. In this critical zone, the average stresses are measured at 141.16 MPa for loading P1 and 204.24 MPa for P2. Furthermore, observations for the VSB show stress contours for each load, P1 and P2, with the region of high stress expanding as the magnitude of the applied load increases. Nevertheless, the calculated values in both cases remain below the material's yield strength. Additionally, it was found that no plastic deformation occurred under either loading condition, as detailed in Tables 6 or 7.

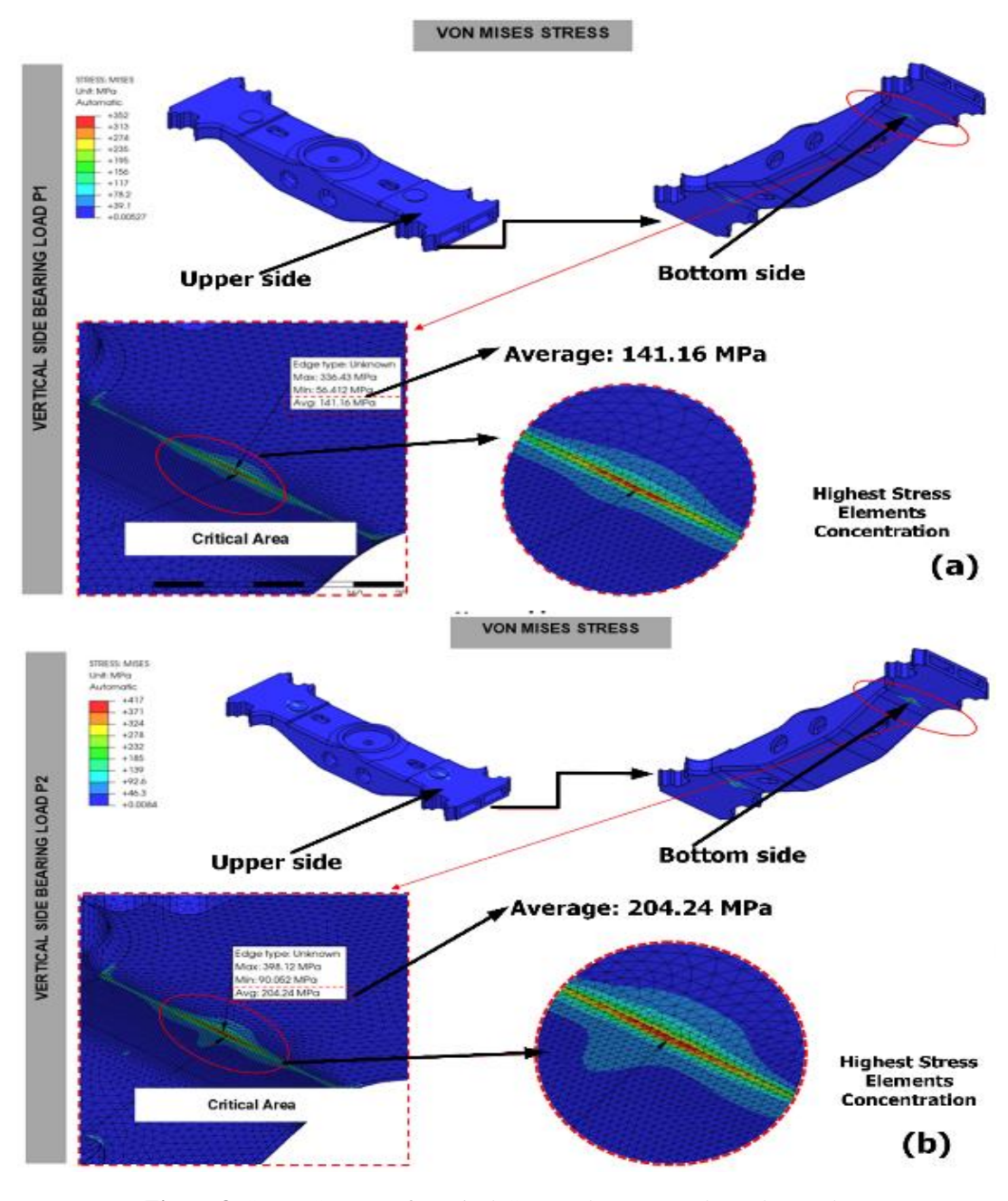


Figure 8. Stress Contour of Vertical Centre Plate (a) Load P1, (b) Load P2

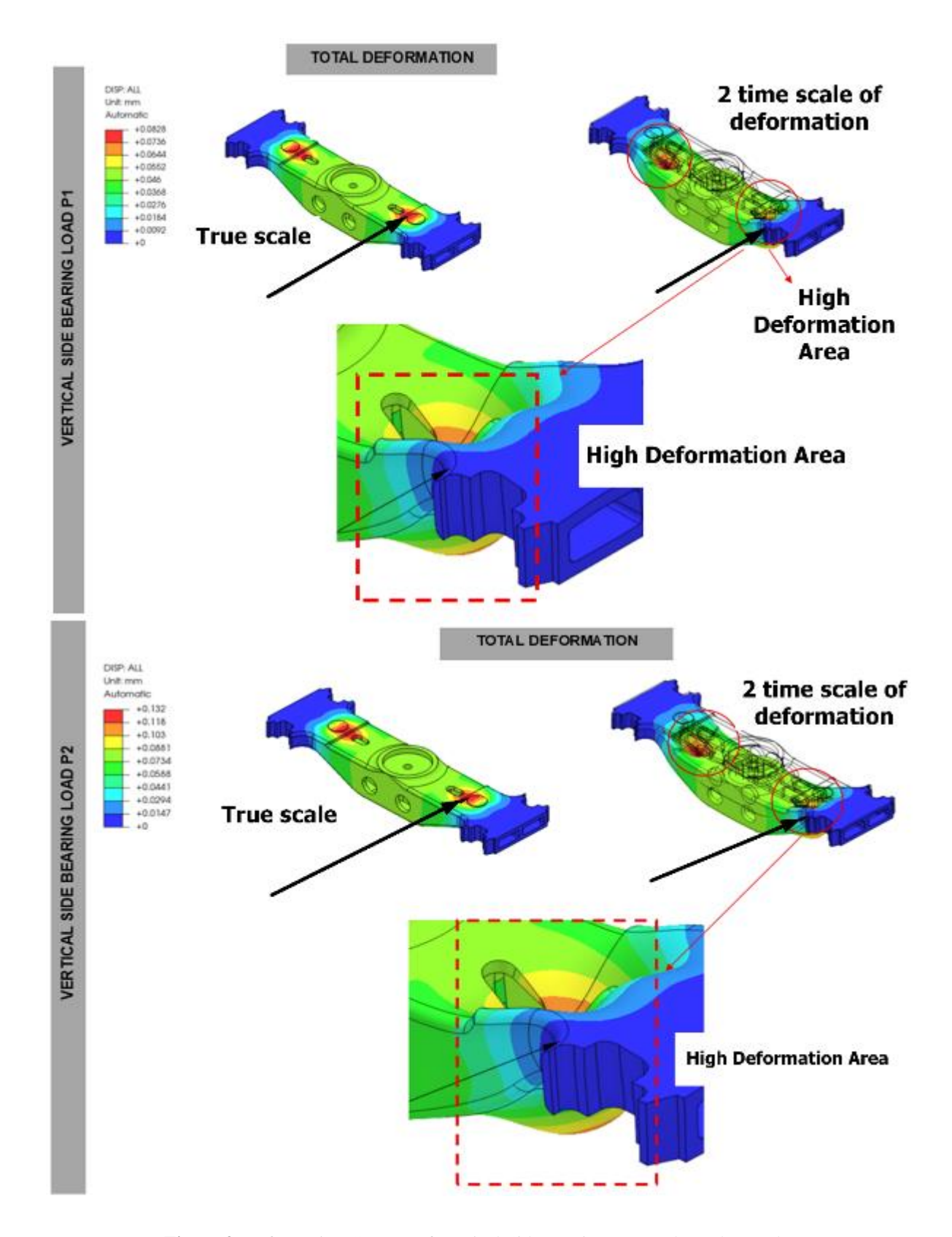


Figure 9. Deformation Contour of Vertical Side Bearing (a) Load P1, (b) Load P2

Figures 9a and b illustrate the deformation contours of the bogie bolster due to vertical loads P1 and P2. The most significant deformation under VSB loading occurs in the bearing side region directly at the point of load application. As loads P1 and P2 increase, the deformation contours expand. This expansion indicates a structural reaction proportional to the magnitude

of the load. Under the loads applied by P1 and P2, the maximum recorded deformation values were for P1, $\delta_{max} = 0.082$ mm, and for P2, $\delta_{max} = 0.132$ mm.

Table 6. Von Mises Stress Results

Code	Load (N)	$\sigma_{\gamma} \ (ext{MPa})$	σ _{avg} (MPa)			
Vertical Centre Plate						
P1	536010.7	200	196.09			
P2	1027500	390	305.58			
Vertical Side Bearing						
P1	536010.7	390	141.16			
P2	854058.5	390	204.24			

Table 7. Total Deformations Results

Code	Load (N)	δ_{max} (mm)	δ _{Allowable} (mm)			
Vertical Center Plate						
P1	536010.7	0.482 (elastic)	2.667 (elastic)			
P2	1027500	0.926 (elastic)	0.635 (plastic)			
Vertical Side Bearing						
P1	536010.7	0.082 (elastic)	1.778 (elastic)			
P2	854058.5	0.132 (elastic)	0.635 (plastic)			

Table 7 shows that plastic deformation did not occur in any loading scenario from P1 to P2. This is also evident in the deformation contours under VCP and VSB loading conditions, where the stress level in the peak deformation region was below the material's yield strength σ_{γ} . This indicates that the bearing structure remained within the elastic range under all applied loading levels.

CONCLUSION

An examination of the vertical load on the central plate and side bearings of the railroad bogie structure has been performed. The stress and deformation analysis of the structure was conducted using Finite Element Analysis (FEA) with a converging mesh and an element size of 2. The simulation findings from the Vertical Center Plate (VCP) and Vertical Side Bearing (VSB) indicate that the bolster constructed from ASTM A148 Grade 80-50 material exhibits commendable mechanical performance under static loading conditions. The critical stress region shows that as the applied load increases, the high-stress zone expands progressively, yet it does not exhibit any indicators of concentration that may suggest a failure risk. Under VCP and VSB loading conditions, the average stress (σ_{avg}) in the critical stress region for loads P1 and P2 remains below the yield strength (σy) of ASTM A148 Grade 80-50 material, which is capped at 305.58 MPa. These observations suggest that the bearings remain within the elastic range under all stress conditions, indicating that no permanent deformation or structural failure is anticipated. This conclusion supports the notion that ASTM A148 Grade 80-50 is a suitable material for bearings exposed to significant static stresses due to its high yield and tensile strength. The existing pillow design meets the mechanical strength and safety criteria established by the AAR M-202 standard. The selection of appropriate materials, adequate structural rigidity, and uniform stress distribution under static loading conditions demonstrate that the bolster component is sufficiently reliable for rail applications. The research concludes that the choice of material standards is a critical factor in the design of a railroad bogie structure for its specific application. Furthermore, the selection of material standards will help mitigate excessive deformation of the bogie, thereby ensuring safety and comfort. It is recommended that dynamic and fatigue analyses be conducted to further verify the reliability of the bearings under these operational conditions.

ACKNOWLEDGMENTS

The authors acknowledge the Institute of Research and Community Service (LPPM) at Universitas Udayana for its support in developing this article under the MBKM research program. We also thank PT INKA, which has supported the CAD laboratory for the successful research and this article.

REFERENCES

- [1] A. W. Evans, "Fatal train accidents on Europe's railways: An update to 2019," *Accid Anal Prev*, vol. 158, p. 106182, Aug. 2021, doi: 10.1016/j.aap.2021.106182.
- [2] S. Zhu, C. Cai, and W. Zhai, "Interface Damage Assessment of Railway Slab Track Based on Reliability Techniques and Vehicle-Track Interactions," *J Transp Eng*, vol. 142, no. 10, Oct. 2016, doi: 10.1061/(ASCE)TE.1943-5436.0000871.
- [3] G. Cai, J. Zhao, Q. Song, and M. Zhou, "System architecture of a train sensor network for automatic train safety monitoring," *Comput Ind Eng*, vol. 127, pp. 1183–1192, Jan. 2019, doi: 10.1016/j.cie.2018.04.038.
- [4] N. Wang, X. Yang, J. Chen, H. Wang, and J. Wu, "Hazards correlation analysis of railway accidents: A real-world case study based on the decade-long UK railway accident data," *Saf Sci*, vol. 166, p. 106238, Oct. 2023, doi: 10.1016/j.ssci.2023.106238.
- [5] B. Dorsey, M. Olsson, and L. J. Rew, "Ecological Effects of Railways on Wildlife," in *Handbook of Road Ecology*, Wiley, 2015, pp. 219–227. doi: 10.1002/9781118568170.ch26.
- [6] S. Qu, J. Wang, D. Zhang, D. Li, and L. Wei, "Failure analysis on bogic frame with fatigue cracks caused by hunting instability," *Eng Fail Anal*, vol. 128, p. 105584, Oct. 2021, doi: 10.1016/j.engfailanal.2021.105584.
- [7] J. Tittel, M. Kepka, and P. Heller, "Static and dynamic testing of a bogie," *IOP Conf Ser Mater Sci Eng*, vol. 723, p. 012031, Feb. 2020, doi: 10.1088/1757-899X/723/1/012031.
- [8] B. Li and Q. Li, "Coupled FEM-DEM modelling of permeability evolution in rough fractured shale during shearing under varying confining pressures," *Journal of Rock Mechanics and Geotechnical Engineering*, Apr. 2025, doi: 10.1016/J.JRMGE.2025.03.017.
- [9] P. A. Dhaware and G. Arunkumar, "Experimental Investigation and Fatigue Analysis of Primary Suspension Spring of Railway Bogies: A Review," *Techno-Societal 2018 Proceedings of the 2nd International Conference on Advanced Technologies for Societal Applications*, vol. 2, pp. 951–963, 2020, doi: 10.1007/978-3-030-16962-6 94.
- [10] J. L. San Román, C. Álvarez-Caldas, and A. Quesada, "Structural Validation of Railway Bogies and Wagons Using Finite Elements Tools," *Proc Inst Mech Eng F J Rail Rapid Transit*, vol. 219, no. 3, pp. 139–150, May 2005, doi: 10.1243/095440905X8844.
- [11] N. S. Ottosen and H. Petersson, *Introduction to the Finite Element Method*. 1992.
- [12] W. Zhao and Y. Zeng, "Comparative study of static strength and fatigue strength tests and simulation analysis of an exit subway bogic frame," in *Third International Conference on Mechanical Design and Simulation (MDS 2023)*, M. A. Mellal and Y. Rao, Eds., SPIE, Jun. 2023, p. 47. doi: 10.1117/12.2681869.
- [13] J. Gerlici, G. Vatulia, A. Lovska, Ye. Krasnokutskyi, and S. Solcansky, "The research into the vertical dynamics of the flat wagon loaded with hopper container with consideration of their

- elastic interaction," *Transportation Research Procedia*, vol. 74, pp. 395–402, 2023, doi: 10.1016/j.trpro.2023.11.160.
- [14] D. Hu, X. Jin, C. Yang, and H. Wang, "Strength analysis of subway bogic frame based on experiment," in *Seventh International Conference on Traffic Engineering and Transportation System (ICTETS 2023)*, A. R. Ghanizadeh and H. Jia, Eds., SPIE, Feb. 2024, p. 188. doi: 10.1117/12.3016113.
- [15] J. L. San Román, C. Álvarez-Caldas, and A. Quesada, "Structural Validation of Railway Bogies and Wagons Using Finite Elements Tools," *Proc Inst Mech Eng F J Rail Rapid Transit*, vol. 219, no. 3, pp. 139–150, May 2005, doi: 10.1243/095440905X8844.
- [16] P. Shahidi, D. Maraini, B. Hopkins, and A. Seidel, "Estimation of Bogie Performance Criteria Through On-Board Condition Monitoring," *Annual Conference of the PHM Society*, vol. 6, no. 1, Sep. 2014, doi: 10.36001/phmconf 2014.v6i1.2515.
- [17] J. Dižo, J. Harušinec, and M. Blatnický, "Computation of Modal Properties of Two Types of Freight Wagon Bogie Frames Using the Finite Element Method," *Manufacturing Technology*, vol. 18, no. 2, pp. 208–214, Apr. 2018, doi: 10.21062/ujep/79.2018/a/1213-2489/MT/18/2/208.
- [18] I. Blanari and V. Goanta, "Stress/Strain analysis in the bogie in linear motion," *IOP Conf Ser Mater Sci Eng*, vol. 564, no. 1, p. 012048, Oct. 2019, doi: 10.1088/1757-899X/564/1/012048.
- [19] S. David Müzel, E. P. Bonhin, N. M. Guimarães, and E. S. Guidi, "Application of the Finite Element Method in the Analysis of Composite Materials: A Review," *Polymers (Basel)*, vol. 12, no. 4, p. 818, Apr. 2020, doi: 10.3390/polym12040818.
- [20] Y. P. D. S. Depari *et al.*, "Numerical analysis of static loading on bogie frame of the Indonesian High-Speed Train (HST) using EN 13749 with 7 load cases," 2024, p. 020048. doi: 10.1063/5.0205924.
- [21] S. D. Iwnicki, S. Stichel, A. Orlova, and M. Hecht, "Dynamics of railway freight vehicles," *Vehicle System Dynamics*, vol. 53, no. 7, pp. 995–1033, Jul. 2015, doi: 10.1080/00423114.2015.1037773.
- [22] S. Wang, P. Wu, Y. Song, C. Liu, Y. Ye, and F. Li, "Vibration environment spectrum investigation of metro bogie frame end," *Eng Fail Anal*, vol. 157, p. 107865, Mar. 2024, doi: 10.1016/j.engfailanal.2023.107865.
- [23] AAR, "AAR Section S Edition," *The Association of American Railroads*, 50 F Street, N.W., Washington, D.C. 20001-1564, 2007.
- [24] R. D. Cook, "Concepts and applications of finite element analysis," *John Wiley & Sons*, 2001.
- [25] I Nyoman Budiarsa, IDG Ary Subagia, I Wayan Widhiada, and Ngakan PG Suardana, "Characterisation of material parameters by reverse finite element modelling based on dual indenters Vickers and spherical indentation," *Procedia Manuf*, vol. 2, 2015.
- [26] S. K. Sharma and A. Kumar, "Dynamics Analysis of Wheel Rail Contact Using FEA," *Procedia Eng*, vol. 144, pp. 1119–1128, 2016, doi: 10.1016/j.proeng.2016.05.076.
- [27] B. M. Nickerson, "Development of an integrated numerical method for the fatigue analysis of railway bogies," 2017.
- [28] J. N. Reddy, An introduction to the finite element method. 1993.
- [29] Y. Wang, J. Xue, X. Zhang, and L. Chen, "Finite Element Analysis and Evaluation of Bogie Frame for Passenger Locomotive based on Reliability," *International Journal of Performability Engineering*, vol. 15, no. 1, p. 146, 2019, doi: 10.23940/ijpe 19.01.p15.146155.
- [30] N. Tao, A. G. Anisimov, and R. M. Groves, "FEM-assisted shearography with spatially modulated heating for non-destructive testing of thick composites with deep defects," *Compos Struct*, vol. 297, p. 115980, Oct. 2022, doi: 10.1016/j.compstruct.2022.115980.
- [31] H. Cui *et al.*, "Destructive testing and simulation for newly designed full-scale high-speed railway box girder," *Constr Build Mater*, vol. 328, p. 127112, Apr. 2022, doi: 10.1016/j.conbuildmat.2022.127112.
- [32] A. Kerebih Jembere, V. Paramasivam, S. Tilahun, and S. K. Selvaraj, "Stress analysis of different cross-sections for passenger truck chassis with a material of ASTM A148 Gr 80–50," *Mater Today Proc*, vol. 46, pp. 7304–7316, 2021, doi: 10.1016/j.matpr.2020.12.985.